Chemically Induced Water Repellency and the Freeze–Thaw Durability of Soils

Masrur Mahedi, Ph.D., A.M.ASCE[1]; Sajjad Satvati, S.M.ASCE[2]; Bora Cetin, Ph.D., M.ASCE[3]; and John L. Daniels, Ph.D., F.ASCE[4]

Abstract: Organosilane (OS) is a silicon-based coupling agent capable of producing hydrophobicity in soils. This study evaluated the applicability of OS in reducing the freeze–thaw impacts on subgrade soils. A frost-susceptible soil was treated with two different dosages (50% and 100% by weight) of 10% OS solution. The OS-treated soils were dried and incorporated into natural soil as layers of 2.5 and 5 cm thickness. The freeze–thaw performances of natural and OS-incorporated soils were then evaluated in terms of maximum frost heave, heave rate, soil moisture distribution, and temperature profile. The OS-treated soil layers decreased frost heaving by 48%–74%. The heave rate of untreated soil was 13.8 cm/day, which was decreased to 4 mm/day with an incorporation of 5 cm-thick layer of 50% OS-treated soil. A 5 cm–50% OS-treated layer was found to be more efficient compared to a 5 cm–100% OS-treated layer in improving the freeze–thaw performance of the soils. **DOI: 10.1061/(ASCE)CR.1943-5495.0000223**. *© 2020 American Society of Civil Engineers.*

Author keywords: Freeze–thaw; Organosilane; Hydrophobicity; Frost heaving; Subgrade soil.

Downloaded from ascelibrary.org by John Daniels on 07/21/20. Copyright ASCE. For personal use only; all rights reserved.

Introduction

Frost heaving and thaw weakening cause substantial damage to pavement subgrade soils in cold regions throughout the world, including large swaths of the United States, Canada, northern Europe, Russia, and China. These cold regions could be classified as permafrost, where the ground remains frozen throughout the year, or as seasonally frozen areas (Zeinali et al. 2016). In particular, pavements in seasonally frozen areas undergo considerable amounts of deteriorations due to frost heaving and thaw weakening (Cetin et al. 2019). During cold weather, when the subsurface temperature drops below 0°C, a fraction of the soil water is crystallized into ice, causing the initial stages of heave (Rosa et al. 2017). Heaving becomes significant as water migrates toward the frozen fringe from the underlying unfrozen zones, freezes, and expands lenses of ice (Johnson 2012). In spring, temperature increases from the surface and the ice crystals in the uppermost layers melts. This melted water becomes trapped by the underlying still-frozen layers, causing substantial loss in bearing capacity of the pavement foundation soils (Simonsen and Isacsson 1999). If the pavement is subjected to traffic during this period, saturated subgrade soils may pump up through the points of least resistance, causing frost-boil issues on the pavement surface (Isotalo 1993). To preclude the pavement damage during the spring thaw, spring load restrictions (SLRs) are often implemented by defining the permissible gross vehicle weight for a given road. However, SLRs are proven to be detrimental to the economy, due to an increase in vehicle number and/or rerouting (Kestler et al. 2007; Levinson et al. 2005; Satvati et al. 2019). In the United States, more than 70% of the road networks are low-volume roads and nearly half of these roads are located in seasonal frozen areas (Kestler et al. 2011). Low-volume roads are known to be susceptible to frost heaving and thaw weakening, since these roads are often made of low-quality materials and are frequently subject to heavy agricultural traffic loads (Coghlan 2000).

Techniques such as crushed-rock interlayer (CRI), two-phase closed thermosyphon (TPCT), and chemical stabilization have been widely used to reduce the freeze–thaw impacts on pavement subgrade soils. However, none of these techniques has proven to be a long-term solution in mitigating the freeze–thaw impacts. CRI performances are known to be adversely effected by clogging, soil deposition, snow covering, and changes in temperature-boundary conditions (Chen et al. 2018; Lepage et al. 2012). TPCT performances fluctuate and are reported to be discontinuous in a single operation phase (Wang et al. 2005). Soil treatment with cement, lime, asphalt, and fly ashes could provide insulation to freeze–thaw, but the chemical stabilizations may lose their efficacy over time due to recurrent moisture intrusion, frost heaves, and thaw settlements phases (Rosa et al. 2017; Shibi and Kamei 2014). Moisture damage or stripping, and subsequent reduction in strength and stiffness properties are the major concerns for asphalt treatments (Hossain et al. 2015; Khan et al. 2018). In addition, higher amounts of chemical stabilizers are required to treat frost-susceptible soils, which increases the overall construction costs (Sargam et al. 2020). Mahedi et al. (2019a) evaluated the prospective use of phase-change materials (PCM) in reducing the sessional temperature variations by harnessing the latent heat of fusion (Mahedi et al. 2019a). However, loss in compressive strength and leakage are constraining the use of PCM in amending the freeze–thaw performance of soils. Hence, an effective and novel alternative is required to mitigate the freeze–thaw impacts on pavement foundation soils.

[1]Postdoctoral Research Associate, Dept. of Civil, Construction and Environmental Engineering, Iowa State Univ., 813 Bissell Rd., Ames, IA 50011. Email: mmahedi@iastate.edu

[2]Graduate Research Assistant, Dept. of Civil, Construction and Environmental Engineering, Iowa State Univ., 813 Bissell Rd., Ames, IA 50011. Email: ssatvati@iastate.edu

[3]Assistant Professor, Dept. of Civil and Environmental Engineering, Michigan State Univ., 428 S. Shaw Ln., East Lansing, MI 48824 (corresponding author). Email: cetinbor@msu.edu

[4]Professor and Chair, Dept. of Civil and Environmental Engineering, Univ. of North Carolina at Charlotte, Charlotte, NC 28223. Email: jodaniel@uncc.edu

Note. This manuscript was submitted on November 5, 2019; approved on March 6, 2020; published online on June 8, 2020. Discussion period open until November 8, 2020; separate discussions must be submitted for individual papers. This paper is part of the ***Journal of Cold Regions Engineering***, © ASCE, ISSN 0887-381X.

Three conditions are required to form ice lenses in soils: subfreezing temperature, frost-susceptible soils with capillary action, and water supply to the frost fringe from a high groundwater table or other source of water (Johnson 2012). It was theorized that excluding the supply of water to the frost fringe could be the most effective solution in reducing the freeze–thaw impacts on subgrade soils. To investigate this, in the current study, soil was treated with organosilane (OS), a silica-based organic coupling agent to induce hydrophobicity. OS could permanently modify the soil surface by grafting organic molecules without rendering any interparticle bonding (Daniels et al. 2009). Thus, the soil particles demonstrate water-repellency properties with a coated layer of organic molecules through covalent bonding mechanisms (Feyyisa et al. 2017). An increase in soil hydrophobicity could decrease the migration of water toward the frost front, which would potentially negate the freeze–thaw impacts. Previous studies indicated substantial decreases in water infiltration capacity and an increase in water-entry pressure in soils due to OS treatment (Daniels et al. 2009; Daniels and Hourani 2009). Therefore, an experimental program was formulated to evaluate the implication of OS in reducing the freeze–thaw impacts on pavement subgrade soils. A frost-susceptible soil was modified by creating 2.5 and 5 cm-thick OS-treated soil layers within a given specimen. The freeze–thaw performance of OS-treated and untreated soils specimens was evaluated by applying frost-heave and thaw-weakening susceptibility tests. Continuous measurements on frost heave and thaw settlement of the prepared specimens were performed by laser-displacement transducers. In addition, each specimen was equipped with six thermocouples to monitor the temperature profile throughout the test period.

Materials

For the experimental program of this study, a frost-susceptible soil was collected in 20-gallon bins from the loess hills in western Iowa. The particle size distribution of the soil was performed in accordance with ASTM C136/C136M (ASTM 2014a). About 98% of the soil passed through U.S. No. 200 (<0.075 mm) sieve (Fig. 1). The liquid limit (LL) and plasticity index (PI) of the soil were determined to be 24 and 4, respectively (ASTM D4318, ASTM 2017b). According to the Unified Soil Classification System (USCS), the soil was classified as low-plasticity silt (ML) (ASTM D2487, ASTM 2017a). The AASHTO classification of the soil was A-4 (AASHTO M145-91, AASHTO 2009). The compaction characteristics of the soil were determined in accordance with ASTM D698 (ASTM 2012). The optimum moisture content and maximum dry density of the soil were 16.2% and 16.67 kN/m^3, respectively. In addition, the specific gravity (G_s) of the soil particles was 2.64 (ASTM D854, ASTM 2014b). Table 1 provides all the measured physical properties of the soil. The chemical composition of the soil was determined by X-ray fluorescence spectrometry (XRF) and is reported in Table 1. The soil was primary composed of silica and alumina, with the presence of basic oxides (CaO, MgO, SrO, Na_2O, and K_2O). A small amount of lime (CaO) and magnesium oxide (MgO) was identified, which made the soil slightly alkaline. The pH of the soil was 8.6, as determined by ASTM D4972 (ASTM 2013b). The loss on ignition (LOI) of the soil was 6.91, indicating the presence of organic materials. In a separate study, the dissolved organic carbon concentration from the soil was determined to be 0.78 mg/L at soil pH of 8.6 (Mahedi et al. 2019b).

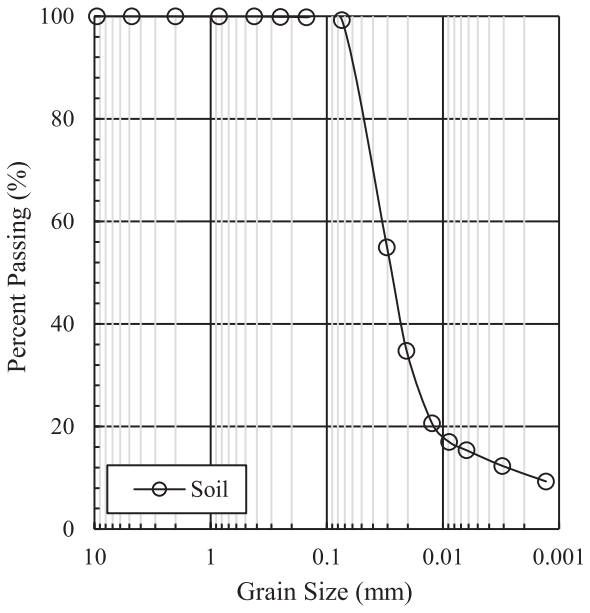

Fig. 1. Particle size distribution of the soil used in this study.

The OS used in this study was heat stable, transparent, and initially water soluble. The commercial name of the OS was TerraSil, and was purchased from Zydex Industries, India. The physical appearance of the OS was pale-yellow and had a density of 1.01 g/mL at room temperature. The freezing temperature and the flashpoint of the OS were reported to be 5°C and 80°C, respectively. Chemically, the used OS was a mixture of ethylene glycol, benzyl alcohol, and hydroxyalkyl-alkoxy-alkyl (Pandagre and Rawat 2016). The OS was reactive and modified the soil surface by converting the soil hydroxyl groups to water-resistant alkylsiloxane. Thus, a permanent 4–6 nm-thick hydrophobic layer was formed which induced the water repellency properties in soil particles.

Methods

To evaluate the frost-heave and thaw-weakening susceptibility of OS-treated and untreated soils, freeze–thaw assessment was performed in accordance with ASTM D5918 (ASTM 2013a). The collected soil was divided into small batches, as per ASTM C702/C702M (ASTM 2018). Soil batches were further reduced to 5 kg small subbatches, following an alternative quartering method to ensure homogeneity between the batches. The collected soil was first placed on a polyethylene sheet and mixed thoroughly by turning the entire sample three times. Following mixing, the whole soil sample was shoveled into a conical pile. Next, the pile

Table 1. Physical and chemical properties of the soil used in this study

Soil physical properties		Soil chemical properties[a]	
Silt content (%)	87	CaO	5.2
Clay content (%)	11	SiO_2	67.7
Liquid limit (LL) (%)	24	Fe_2O_3	3.3
Plasticity index (PI) (%)	4	Al_2O_3	9.6
Specific gravity (G_s)	2.64	MgO	2.1
Optimum moisture (%)	16.2	K_2O	2.06
Maximum dry density (kN/m^3)	16.67	SO_3	0.03
USCS classification	ML	pH	8.6
AASHTO classification	A-4	LOI (%)	6.91

Note: Clay content <0.002 mm; Silt content = 0.075–0.002 mm; LOI = loss on ignition; and pH = following ASTM D4972 (ASTM 2013b).
[a]X-ray fluorescence analysis.

Downloaded from ascelibrary.org by John Daniels on 07/21/20. Copyright ASCE. For personal use only; all rights reserved.

was flattened to uniform thickness and diameter by pressing down the apex with a shovel. The flattened mass was then divided into four equal quarters and the soil from two diagonally opposite quarters were removed. The remaining soil was successively mixed and divided until the sample size was reduced to 5 kg. Afterward, the reduced subbatches were oven dried, wetted with the optimum amount of water (16.2%), and mixed thoroughly. Next, the soil was compacted in six layers by using a laboratory-customized mold and a Proctor compaction hammer. Six acrylic disks and a latex membrane were provided for each specimen to facilitate the test setup and saturation. The size of the prepared specimens was 14.6 cm in diameter and 15.2 cm in height.

The same preparation procedure was followed both for OS-treated and untreated specimens. For treated specimens, the OS-modified soil layers were incorporated at two depths: 5.1–7.6 cm and 5.1–10.1 cm. For treating the soil with OS, a water–OS solution was prepared by mixing 10 parts of distilled water for every part of OS (10% OS solution). Next, the 10% OS solution was added to oven-dried soil at the rates of 50% and 100% by weight (1:2 and 1:1 ratios), and air dried, following the procedure described in Daniels et al. (2009). The 50% OS-treated soil was incorporated in freeze–thaw specimens as 2.5 and 5 cm-thick layers at the aforementioned depths. The 100% OS-treated soil was fused only as a layer of 5 cm at a depth of 5.1–10.1 cm. To fuse OS-treated soil layers in the specimens, first natural soil was compacted in two layers up to a height of 5.1 cm. Next, a layer of OS-treated soil was placed and compacted to a height of 7.6 cm. In the case of 2.5 cm 50% OS-sandwiched soil specimen, the remaining three layers were compacted by using natural soil. For 5 cm 50% and 100% OS-sandwiched specimens, an additional OS-treated soil layer was compacted at a height of 7.6–10.1 cm, and the remaining two layers were packed with natural soil. All the layers were compacted by implementing 33 blows using a Proctor hammer. All the prepared specimens were then saturated for 24 h following the pressure-head schedule outlined in ASTM D5918 (ASTM 2013a).

Tests were performed in a cooling chamber at a constant temperature of 3°C. Two heat-exchangers were placed at the top and bottom of each of the specimens to apply freezing and thawing cycles. Freezing was initiated by lowering the top heat-exchanger temperature to −3°C and −12°C simultaneously, and fixing the bottom heat-exchanger temperature to +3°C and 0°C, sequentially. During the thawing period, the top and bottom heat-exchanger temperatures were elevated to +12°C and +3°C, respectively. The temperature of the heat-exchangers was controlled by two separate programmable temperature-control baths manufactured by PolyScience. The operating range of the control baths was −30°C to +200°C, with a stability of ±0.01°C. Following ASTM D5918 (ASTM 2013a), two freezing and thawing cycles were applied sequentially for a duration of 120 h. ASTM D5918 (ASTM 2013a) adopted the test method developed by Chamberlain (1986). Chamberlain (1986) implemented two freeze–thaw cycles, concluding that, except for clay soils, most of the structural changes of soils affecting heave rate occurs during the first cycle. Therefore, two freeze–thaw cycles were implemented to make the test more readily available, which was also accepted by ASTM D5918 (ASTM 2013a). Table 2 provides a summary of the test schedule. In addition, to simulate the groundwater table, water was supplied to the specimens through the bottom plates at a constant pressure head of 1.27 cm.

Laser-displacement transducers were used to measure the frost heaving and thaw settlement during the test progress. The laser had a resolution of 0.75 μm at a measurement range of 50 mm. To measure the temperature variations across the length of the specimens, each specimen was equipped with six thermocouples at a depth of 1.3, 3.8, 6.4, 8.9, 11.4, and 14 cm from the top. A type T thermocouple with a data acquisition system was use. The type T thermocouple had a measurement range of −200°C to +500°C, with an accuracy of ±1.8°C. The data acquisition system recorded the temperatures at six different depths and the displacement at the top of the specimens at one-minute intervals. Fig. 2 shows the idealized test setup arranged in this study. As shown in Fig. 2(a), four samples were assembled in the cooling chamber at a temperature of 3°C. A surcharge load of 5.5 kg was placed on top of each specimen. The laser-displacement transducers were placed 5 cm above

Table 2. Test schedule for frost-heave and thaw-weakening test

Days	Elapsed time (h)	Top plate temperature (°C)	Bottom plate temperature (°C)	Comments
1	0–24	3	3	24 h conditioning
2	24–32	−3	3	First 8 h freezing
	32–48	−12	0	Freeze to bottom
3	48–64	12	3	First thawing
	64–72	3	3	8 h conditioning
4	72–80	−3	3	Second 8 h freezing
	80–96	−12	0	Freeze to bottom
5	96–112	12	3	Second thawing
	112–120	3	3	Final conditioning

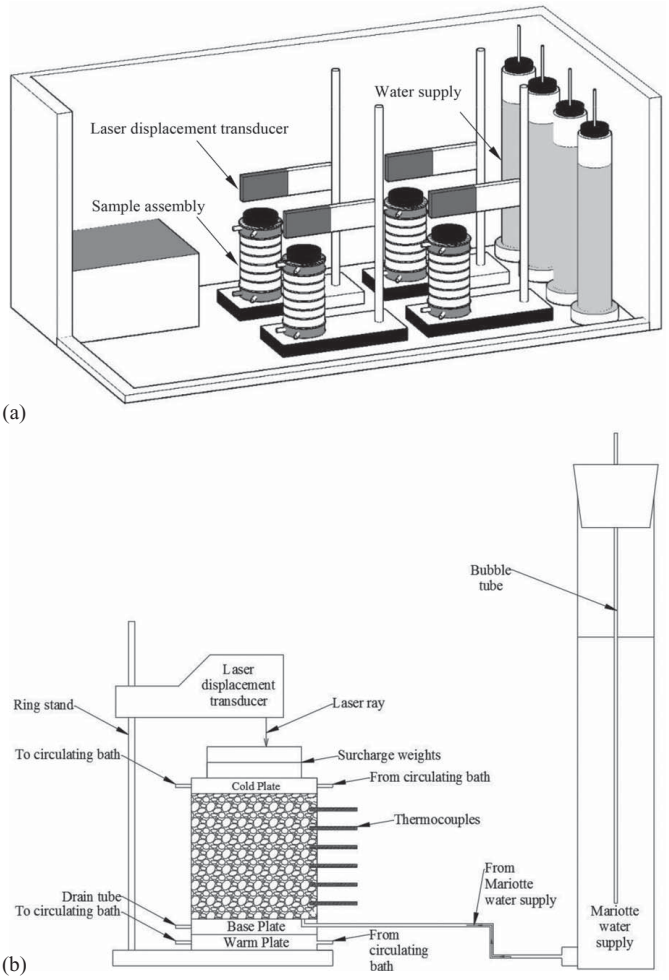

Fig. 2. Frost-heave and thaw-weakening test: (a) freeze cabinet; and (b) sample assembly.

Downloaded from ascelibrary.org by John Daniels on 07/21/20. Copyright ASCE. For personal use only; all rights reserved.

the top of the surcharge load. Separate Marriott bottles were used to supply water to the specimens. The bottoms of the Marriott bottles were connected to the inlet port of the specimen baseplates with flexible tubes [Fig. 2(b)]. Water was supplied to the specimens at a constant pressure head of 1.27 cm by using bubble tubes. Fig. 2(b) shows the approximate locations of the thermocouples.

Results

Heaving Trends and Comparisons

Fig. 3 shows the frost-heave time plots of 2.5 cm–50% OS-, 5 cm–50% OS-, and 5 cm–100% OS-treated and untreated soils. All specimens followed the same trend, where with a decrease in top plate temperature the specimens heaved due to frost penetration, water ingression, and ice lens formation (Johnson 2012). None of the specimens heaved during the first 8 h of freezing period, due to a low freezing temperature (−3°C). The freezing point depression of the soil could be the possible reason for the observed behavior. Previous studies indicated that, depending on moisture content, soil freezes at temperatures lower than 0°C (Kozlowski 2004, 2016). However, the specimens started to swell significantly after 32 h of test progression, when the specimens were frozen to the bottom with a top plate temperature of −12°C. Maximum heaving was observed at the end of the freezing period, with slight association of time lags. Subsequently, thawing was applied by rising the top plate temperature to 12°C, which melted the ice lenses formed during the freezing cycle. As a result, specimens started to consolidate due to phase change and dissipation of absorbed water. However, this process was not completely reversible, resulting in residual or permanent heave.

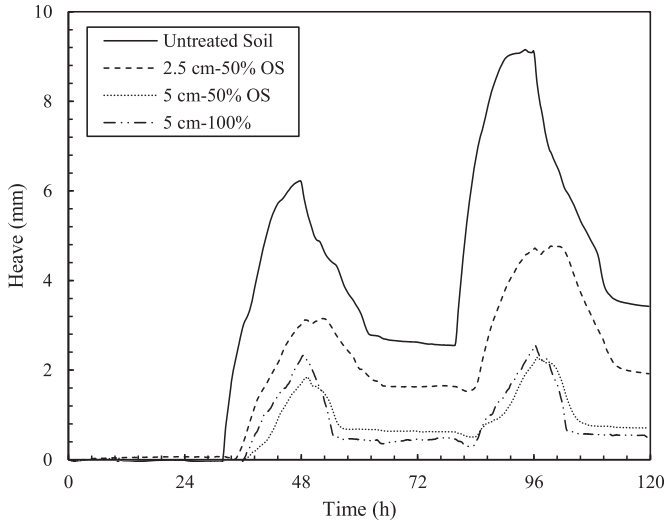

Fig. 3. Frost-heave time plot of OS-treated and untreated soils.

As indicated in Fig. 3, untreated soil started to heave at 32 h of the test progress, whereas OS-treated specimens showed a 2–5 h delayed response to such behavior. A similar observation was also made for the second freezing cycles, where untreated soil heaved after 80 h, but the treated specimens exhibited heaving at around 84 h of test progression. This indicated that OS treatment and the attendant hydrophobicity acted as a barrier to water flow toward the freezing front. As the temperature dropped and the freezing front passed the middle OS-treated layers, water accumulation to the frost fringe was possible and the specimens demonstrated heaving behavior. Nonetheless, the OS-treated specimens showed significantly lower heaving compared to the untreated soil in both freezing cycles.

Fig. 4(a) provides quantitative comparisons of ultimate heaving manifested by each of the treatments along with the untreated soil. The untreated soil heaved to 6.3 mm at the end of first freezing cycles, whereas the maximum heaving for 2.5 cm–50% OS, 5 cm–50% OS, and 5 cm–100% OS treatments were 3.27 mm, 1.9 mm, and 2.4 mm, respectively. The 5 cm–100% OS treatment resulted in higher heaving compared to the 5 cm–50% OS treatment. While not entirely proven, the higher heaving with 100% OS may have occurred because of the test setup and boundary conditions. In particular, more OS translates to less moisture available to freeze. Freezing of water slows down the progression of frost fringe, since water releases heat in the form of latent heat during the phase change (Mahedi et al. 2019a). In the case of the 100% OS, the freezing front may have reached the bottom of the specimen more quickly, resulting in water accumulation beyond the OS-treated zone of this specimen. Water may have then accumulated as an ice layer at the bottom of the specimen, which would explain the increase in overall heaving of the 5 cm–100% OS-incorporated specimen. The lower residual heave of 5 cm–100% OS compared to 5 cm–50% OS treatment (Fig. 3) provides evidence of the explanation. Greater residual heave is observed when the soil water contributes more toward the overall heaving, whereas smaller values

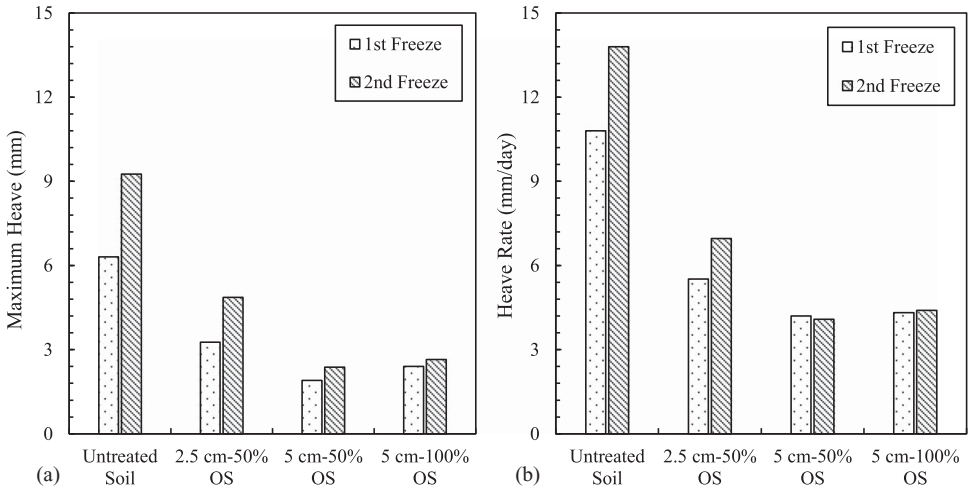

Fig. 4. Frost-heave test result: (a) maximum heave; and (b) heave rate.

Downloaded from ascelibrary.org by John Daniels on 07/21/20. Copyright ASCE. For personal use only; all rights reserved.

are expected when heaving is ensued by ice-layer formation (Mahedi et al. 2019a). This has been further verified by the moisture profile of the specimens, where the 5 cm–100% OS-incorporated soil specimen showed the highest moisture content at a depth of 14 cm. In addition, as indicated in Fig. 4(a), maximum heaving is always higher in the second freezing cycle. This was attributed to an increase in hydraulic conductivity due to the change in soil structure during the first freezing cycle (Chamberlain 1986). The variation in maximum heave in two freezing cycles was less for 5 cm–100% OS-treated soil (<10.5%), since less alteration of soil structure was expected due to small water ingression and minor ice lens formation in 5 cm–100% OS-fused soil.

Fig. 4(b) shows the heave rates of OS-treated and untreated specimens for both the freezing cycles. The heave rates were determined as the tangent of the heave-line, as describe in Zhang et al. (2016). Higher heave rates were associated with untreated soil, whereas heave rates decreased significantly due to OS treatment. Generally speaking, heave rates for the second freezing cycle were higher compared to those found in the first freezing cycle. However, specimens with 5 cm of OS-treated layers showed trivial differences in heave rates, depending on whether it was the first or second freeze cycle. The minimum heave rates were associated with 5 cm–50% OS treatment. ASTM D5918 (ASTM 2013a) provides the frost susceptibility classification based on the second heave rate. As per ASTM D5918 (ASTM 2013a), the frost susceptibility of soils is "high" when the second heave rates are between 8 and 16 mm/day, "medium" if in the range of 4 to 8 mm/day, and "low" for 2 to 4 mm/day of heave rates. As shown in Fig. 4(b), untreated soil showed higher frost susceptibility, with a heave rate of 13.8 mm/day. The frost susceptibility of the soil decreased to medium with an incorporation of a 2.5 cm–50% OS-treated layer (6.96 mm/day). The 5 cm–50% OS and 5 cm–100% OS treatments reduced the frost susceptibility of the soil to low and medium low (4 and 4.4 mm/day for 5 cm–50% OS and 5 cm–100% OS, respectively).

Moisture Profile

At the end of the freeze–thaw tests, each specimen was divided into six 2.54 cm-thick soil layers to assess the soil moisture distribution.

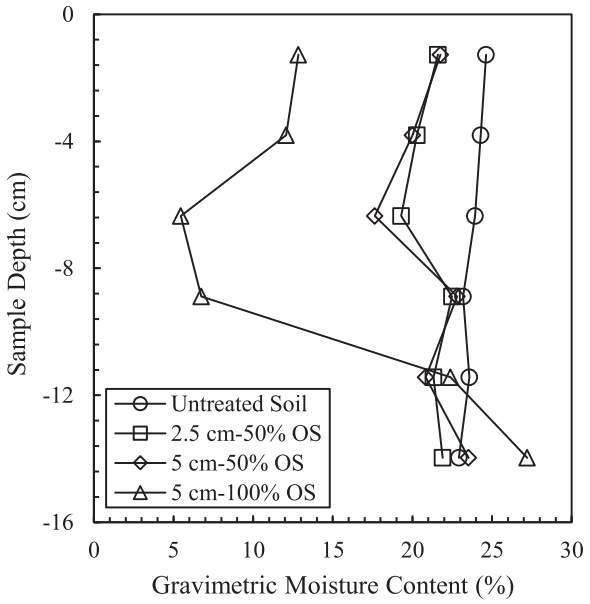

Fig. 5. Moisture profile of the specimens after the end of freeze–thaw cycles.

A moisture sample was taken from the middle of the layers. As seen in Fig. 5, untreated soil showed a gradual increase in moisture content toward the top. Except for the bottom-most layer, untreated soil had the highest moisture contents at every depth. This indicated an upward movement of water toward the freezing front during the freezing cycle. Up to a depth of 6.4 cm, the moisture contents of 50% OS treatments were significantly lower than those of untreated ones. The lowest moisture contents for 50% OS-contained specimens were also found at the depths of 6.4 cm. The 5 cm–50% OS showed lower moisture at this depth compared to the 2.5 cm–50% OS treatment. At depths of 8.9–14 cm, the moisture contents of 50% OS treatments were comparable to the untreated soil. It is significant to note that the OS-treated layers were placed at depths of 5.1–10.1 cm, which acted as a barrier against the upward movement of water. Therefore, moisture contents were lower above the OS treated layers, whereas comparable moisture contents between the treated and untreated specimens were found at depths higher than 8.9 cm. In the case of the 5 cm–100% OS treatment, the lowest moisture contents were associated at depths of 6.4–8.9 cm, in proximity to the OS-treated layer. The drier zone in 5 cm–100% OS-treated soils was extended to 8.9 cm due to the higher water repellency properties of the 100% OS-modified layer. Up to a depth of 8.9 cm, 5 cm–100% OS treatment resulted in the lowest moisture contents compared to the other treated and untreated soils. Yet, 5 cm–100% OS resulted in slightly higher heaves than those from 5 cm–50% OS treatment. This is justified by relatively higher moisture contents of 5 cm–100% OS incorporation at depths higher than 8.9 cm. Apparently, because of less moisture at the top portion of the 5 cm–100% OS-incorporated soil specimen, the freezing front quickly passed the OS layer and accumulated moisture at depths of 10.1–15.2 cm. Among all the prepared specimens, the maximum moisture content was found for the 5 cm–100% OS treatment at a depth of 14 cm, indicating the possible formation of an ice layer.

Temperature Distribution

Fig. 6 shows the spatial and temporal distribution of soil temperatures in OS-treated and untreated specimens. Higher variations in temperature were observed at the top portion of the specimens, whereas the differences in temperatures were less at greater depths. At a certain depth, the OS-incorporated soil showed an immediate decrease or increase in temperature in response to freeze–thaw cycles [Fig. 6(b)]. After the instantaneous changes in temperature, OS-treated specimens sustained a uniform temperature in the rest of the freeze–thaw cycle [Fig. 6(c)]. By contrast, untreated soil showed a delayed, gradual response to freeze–thaw throughout the test period [Fig. 6(a)]. Unlike OS-treated specimens, the maximum and minimum temperatures for untreated soil were observed at the end of a freezing or thawing cycle. The freezing process of water releases a large amount of latent heat, whereas the same amount of heat energy is absorbed in the ice-melting process (Johnson 2012; Zhang et al. 2016). During the freezing cycles of untreated soil, water constantly migrated toward the freezing front, turned into ice, and released the heat of fusion. The process decelerated the downward progression of frost fringe in untreated soils, resulting in a gradual decrease in the temperature (Johnson 2012). In the thawing cycles, the temperature increases for untreated soil was gradual, since the ice lenses continuously absorbed heat to melt into water. In the case of OS-treated soils, the migration of water toward the frost fringe was limited by the enhanced hydrophobicity of soil particles. Therefore, less water was subject to phase transformations, resulting a rapid change in temperature for OS-incorporated soils. Once the phase change of available water

Downloaded from ascelibrary.org by John Daniels on 07/21/20. Copyright ASCE. For personal use only; all rights reserved.

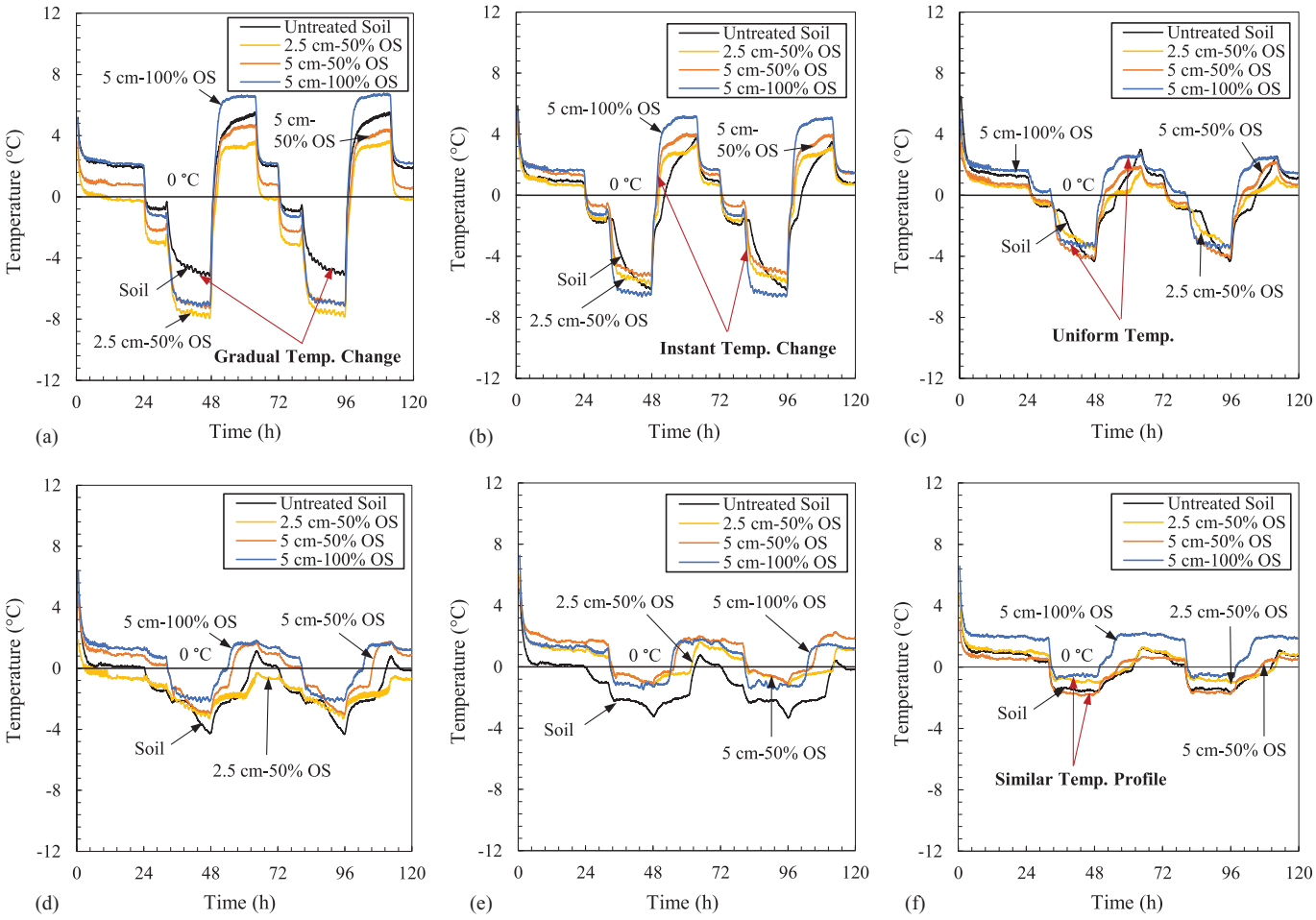

Fig. 6. Temperature profile of the specimens at the depths of: (a) 1.3 cm; (b) 3.8 cm; (c) 6.4 cm; (d) 8.9 cm; (e) 11.4 cm; and (f) 14 cm.

was complete, the temperature became uniform in OS-treated specimens. As the frost fringe extended beyond the OS layers, the differences between the treated and untreated soil specimens were reduced, as indicated in Figs. 6(e and f). At greater depths (14 cm), the 5 cm–100% OS-incorporated soil was found to be warmer, which could be because of higher moisture content at that zone (Fig. 5).

Conclusions

This study was conducted to evaluate the freeze–thaw performances of OS-incorporated frost-susceptible soil. Silica-based 10:1 OS solution was used to treat the soil at the addition rates of 50% and 100% by weight. Layers of 2.5 and 5 cm OS-treated soils were sandwiched in between natural soil layers. The freeze–thaw susceptibility of OS-treated and untreated soils were evaluated. Based on the experimental study, the key findings of this study are summarized as follows:

- The treatment of soils with OS and subsequent increase in soil hydrophobicity significantly decreased the frost heaving of the soil. The frost susceptibility classification of untreated soil was "high," which decreased to "medium" or "low" due to OS-treated layers.
- The reduction in maximum heave and heave rates were the highest for the 5 cm–50% OS layer compared with the other treated and untreated specimens.
- The untreated soil showed a steady increase in moisture contents toward the top surface of the specimen. In contrast, OS-treated layers acted as a barrier against the flow of water and precluded the ingression of water above the OS treatments.
- The temperature profile of the prepared specimens varied due to the presence of OS-treated soil layers. Untreated soil showed gradual changes in temperature, whereas the changes for OS-incorporated soils were instantaneous.
- In brief, this study provides evidences supporting the prospective use of OS in negating the freeze–thaw impacts on subgrade soils. Further research involving the field evaluation of OS-treated soils is recommended for a comprehensive evaluation of the freeze–thaw performances of OS-incorporated soils.

Data Availability Statement

All data, models, and code generated or used during the study appear in the submitted article.

References

AASHTO. 2009. *Classification of soils and soil–aggregate mixtures for highway construction purposes*. AASHTO M145-91. Washington, DC: AASHTO.

Downloaded from ascelibrary.org by John Daniels on 07/21/20. Copyright ASCE. For personal use only; all rights reserved.

ASTM. 2012. *Standard test methods for laboratory compaction characteristics of soil using standard effort (12,400 ft-lbf/ft3 (600 kN-m/m^3))*. ASTM D698. West Conshohocken, PA: ASTM.
ASTM. 2013a. *Standard test methods for frost heave and thaw weakening susceptibility of soils*. ASTM D5918. West Conshohocken, PA: ASTM.
ASTM. 2013b. *Standard test methods for pH of soils*. ASTM D4972. West Conshohocken, PA: ASTM.
ASTM. 2014a. *Standard test method for sieve analysis of fine and coarse aggregates*. ASTM C136/C136M. West Conshohocken, PA: ASTM.
ASTM. 2014b. *Standard test methods for specific gravity of soil solids by water pycnometer*. ASTM D854. West Conshohocken, PA: ASTM.
ASTM. 2017a. *Standard practice for classification of soils for engineering purposes (unified soil classification system)*. ASTM D2487. West Conshohocken, PA: ASTM.
ASTM. 2017b. *Standard test methods for liquid limit, plastic limit, and plasticity index of soils*. ASTM D4318. West Conshohocken, PA: ASTM.
ASTM. 2018. *Standard practice for reducing samples of aggregate to testing size*. ASTM C702/C702M. West Conshohocken, PA: ASTM.
Cetin, B., S. Satvati, J. C. Ashlock, and C. Jahren. 2019. *Performance-based evaluation of cost-effective aggregate options for granular roadways*. Ames, IA: Iowa Highway Research Board.
Chamberlain, E. J. 1986. *Evaluation of selected frost-susceptibility test methods*. Hanover, NH: U.S. Army Cold Regions Research and Engineering Laboratory.
Chen, L., W. Yu, X. Yi, D. Hu, and W. Liu. 2018. "Numerical simulation of heat transfer of the crushed-rock interlayer embankment of Qinghai-Tibet Railway affected by aeolian sand clogging and climate change." *Cold Reg. Sci. Technol.* 155: 1–10. https://doi.org/10.1016/j.coldregions.2018.07.009.
Coghlan, G. T. 2000. *Opportunities for low-volume roads*. Washington, DC: Transportation Research Board.
Daniels, J. L., and M. S. Hourani. 2009. "Soil improvement with organosilane." In *Advances in ground improvement*, edited byJ. Han, G. Zheng, V. R. Schaefer, and M. Huang, 217–224. Reston, VA: American Society of Civil Engineers.
Daniels, J. L., M. S. Hourani, and L. S. Harper. 2009. "Organo-silane chemistry: A water repellent technology for coal ash and soils." In *2009 World of Coal Ash Conf.*, 1–9. Covington, Kentucky: World of Coal Ash.
Feyyisa, J. L., J. L. Daniels, and M. A. Pando. 2017. "Contact angle measurements for use in specifying organosilane-modified coal combustion fly ash." *J. Mater. Civ. Eng.* 29 (9): 04017096. https://doi.org/10.1061/(ASCE)MT.1943–5533.0001943.
Hossain, Z., B. Bairgi, and M. Belshe. 2015. "Investigation of moisture damage resistance of GTR-modified asphalt binder by static contact angle measurements." *Constr. Build. Mater.* 95: 45–53. https://doi.org/10.1016/j.conbuildmat.2015.07.032.
Isotalo, J. L. 1993. *Seasonal truck-load restrictions and road maintenance in countries with cold climate*. Washington, DC: World Bank.
Johnson, A. 2012. "Freeze-thaw performance of pavement foundation materials." *M.S. thesis*, Civil, Construction, and Environmental Engineering, Iowa State Univ., Digital Repository.
Kestler, M. A., R. L. Berg, H. J. Miller, B. C. Steinert, R. Eaton, G. Larson, and J. Haddock. 2011. "Keeping springtime low-volume road damage to a minimum." *Transp. Res. Rec.* 2205 (1): 155–164. https://doi.org/10.3141/2205-20.
Kestler, M. A., R. L. Berg, B. C. Steinert, G. L. Hanek, M. A. Truebe, and D. N. Humphrey. 2007. "Determining when to place and remove spring load restrictions on low-volume roads." *Transp. Res. Rec.* 1989-2 (1): 219–229. https://doi.org/10.3141/1989-67.
Khan, Z. H., H. M. Faisal, and R. A. Tarefder. 2018. "Phase identification and characterization of aging effects in asphaltic materials by nanoindentation testing." *Transp. Geotech.* 17: 154–164. https://doi.org/10.1016/j.trgeo.2018.10.002.
Kozlowski, T. 2004. "Soil freezing point as obtained on melting." *Cold Reg. Sci. Technol.* 38 (2–3): 93–101. https://doi.org/10.1016/j.coldregions.2003.09.001.
Kozlowski, T. 2016. "A simple method of obtaining the soil freezing point depression, the unfrozen water content and the pore size distribution curves from the DSC peak maximum temperature." *Cold Reg. Sci. Technol.* 122: 18–25. https://doi.org/10.1016/j.coldregions.2015.10.009.
Lepage, J. M., G. Doré, D. Fortier, and P. Murchison. 2012. "Thermal performance of the permafrost protection techniques at beaver creek experimental road site, Yukon, Canada." In *Proc., 10th Int. Conf. on Permafrost*, 261–266. Salekhard, Russia: Northern Publisher.
Levinson, D. M., M. O. Marasteanu, V. Voller, I. Margineau, B. Smalkowski, M. Hashami, N. Li, M. Corbett, and E. Lukanen. 2005. *Cost/benefit study of spring load restrictions*. St. Paul, MN: Minnesota Dept. of Transportation.
Mahedi, M., B. Cetin, and K. S. Cetin. 2019a. "Freeze-thaw performance of phase change material (PCM) incorporated pavement subgrade soil." *Constr. Build. Mater.* 202: 449–464. https://doi.org/10.1016/j.conbuildmat.2018.12.210.
Mahedi, M., B. Cetin, and A. Y. Dayioglu. 2019b. "Leaching behavior of aluminum, copper, iron and zinc from cement activated fly ash and slag stabilized soils." *Waste Manage. (Oxford)* 95: 334–355. https://doi.org/10.1016/j.wasman.2019.06.018.
Pandagre, A. K., and A. Rawat. 2016. "Improvement of soil properties using nonchemical-Terrasil: A review." *Int. J. Res.* 3 (19): 31–38.
Rosa, M. G., B. Cetin, T. B. Edil, and C. H. Benson. 2017. "Freeze–thaw performance of fly ash–stabilized materials and recycled pavement materials." *J. Mater. Civ. Eng.* 29 (6): 04017015. https://doi.org/10.1061/(ASCE)MT.1943-5533.0001844.
Sargam, Y., K. Wang, and J. E. Alleman. 2020. "Effects of modern concrete materials on thermal conductivity." *J. Mater. Civ. Eng.* 32 (2): 04020058. https://doi.org/10.1061/(ASCE)MT.1943-5533.0003026.
Satvati, S., J. C. Ashlock, A. Nahvi, C. Jahren, B. Cetin, and H. Ceylan. 2019. "A novel performance-based economic analysis approach: Case study of Iowa low-volume roads." In *Proc., 12th Int. Conf. on Low-Volume Roads*, 207–234. Washington, DC: Transportation Research Board.
Shibi, T., and T. Kamei. 2014. "Effect of freeze–thaw cycles on the strength and physical properties of cement-stabilised soil containing recycled bassanite and coal ash." *Cold Reg. Sci. Technol.* 106–107: 36–45. https://doi.org/10.1016/j.coldregions.2014.06.005.
Simonsen, E., and U. Isacsson. 1999. "Thaw weakening of pavement structures in cold regions." *Cold Reg. Sci. Technol.* 29 (2): 135–151. https://doi.org/10.1016/S0165-232X(99)00020-8.
Wang, S. J., J. B. Chen, and X. M. Huang. 2005. "Numerical simulation of cooling effect for heat pipe subgrade." *J. Traffic Transp. Eng.* 5 (3): 41–46.
Zeinali, A., D. Dagli, and T. Edeskär. 2016. "Freezing-thawing laboratory testing of frost susceptible soils." In *Proc., 17th Nordic Geotechnical Meeting*, 135–151. Reykjavik, Iceland: Icelandic Geotechnical Society.
Zhang, Y., A. E. Johnson, and D. J. White. 2016. "Laboratory freeze–thaw assessment of cement, fly ash, and fiber stabilized pavement foundation materials." *Cold Reg. Sci. Technol.* 122: 50–57. https://doi.org/10.1016/j.coldregions.2015.11.005.

Downloaded from ascelibrary.org by John Daniels on 07/21/20. Copyright ASCE. For personal use only; all rights reserved.